Ceramics International **14** (1988) 199–205

Subsolidus Phase Relationships in Part of the System Si, Al, Ca/N, O

W. Y. Sun, T. S. Yen (D. S. Yan)

Shanghai Institute of Ceramics, Academia Sinica, Shanghai, People's Republic of China

&

T. Y. Tien

The University of Michigan, Ann Arbor, Michigan 48109, USA

(Received 7 September 1987; accepted 22 September 1987)

Abstract: Subsolidus phase relationships in the region bounded by Si_3N_4, SiO_2, $CaSiO_3$, $2CaO.Al_2O_3.SiO_2$, $CaO.Al_2O_3$, Al_2O_3 and β'-$Si_2Al_4O_4N_4(\beta_{60})$ have been studied. A new quinary phase with composition near to $CaO.1{\cdot}33Al_2O_3.0{\cdot}67Si_2N_2O$ (designated as S-phase) and a complete series of solid solution between S-phase and $CaO.2Al_2O_3$ were found. Fourteen compatible tetrahedra, of which five contain S-phase, occur in the region explored. They are as follows: X_1-SiO_2–anorthite–mullite; X_1-anorthite–mullite–Al_2O_3; X_1-anorthite–Al_2O_3–β_{60}; X_1-anorthite–β_{60}–Si_3N_4; X_1-anorthite–Si_3N_4–Si_2N_2O; X_1-anorthite–Si_2N_2O–SiO_2; anorthite–Si_2N_2O–SiO_2–$CaSiO_3$; anorthite–Si_2N_2O–$CaSiO_3$–gehlenite; anorthite–Si_2N_2O–gehlenite–Si_3N_4; S-anorthite–Al_2O_3–β_{60}; S-Al_2O_3-$CaO.2Al_2O_3$–gehlenite; S-Al_2O_3–gehlenite–anorthite; S-gehlenite–anorthite–Si_3N_4; S-anorthite–Si_3N_4–β_{60}.

1 INTRODUCTION

Various metal oxides (e.g. Al_2O_3, Y_2O_3 and MgO) have been proved to be effective additives to promote densification of Si_3N_4 ceramics. Among these, only Al can enter into the lattice of β–Si_3N_4 to form β'–sialon with oxygen replacing nitrogen simultaneously, while the other oxides always react with the SiO_2 existing at the surface of Si_3N_4 grains and other impurities to form a glassy phase at the grain boundaries, which impairs the high-temperature mechanical properties of Si_3N_4 ceramics. In order to crystallize out this glassy phase as second crystalline phases at the grain boundaries, it is necessary to know the subsolidus relationships in the Si, Al, M/N, O systems (where M represents metal atoms). For instance, the subsolidus relationships in the system Si, Al, Y/N,O have shown that garnet ($3Y_2O_3.5Al_2O_3$) can be formed as a crystalline second phase of the grain boundaries.[1–3] In fact, β'-YAG ceramics with high strength at temperatures in excess of 1000°C have been developed. Calcium is one of the common impurities present in Si_3N_4 powder, which persists at the grain boundaries in Si_3N_4 ceramics in the form of glassy phase. So, it is felt necessary to study the subsolidus phase equilibrium in the system Si, Al, Ca/N, O in order to develop β-Si_3N_4-based ceramics from a lower quality Si_3N_4 powder containing Ca as the main impurity. The compositions investigated were restricted to the region bounded by Si_3N_4, SiO_2, $CaSiO_3$, $2CaO.Al_2O_3.SiO_2$, $CaO.Al_2O_3$, Al_2O_3

Ceramics International 0272-8842/88/$03·50

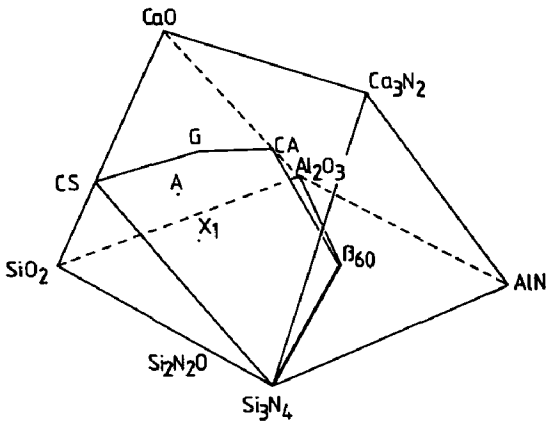

Fig. 1. The Jänecke prism for Ca-sialon system showing the region studied.

and β_{60}, as shown in Fig. 1, which was considered to involve Ca-containing compounds that may coexist with Si_3N_4 and β'-sialon and is more relevant to what we would like to focus upon.

2 EXPERIMENTAL

The starting powders used were silicon nitride (AME, UK, containing 1·3% oxygen), aluminum nitride (Tokyo Shibaura Electric Co., Japan, containing 1·4% oxygen), calcium oxide (calcined calcium carbonate, >99·9%), aluminum oxide (decomposed ammonia alum, >99·9%) and silicon oxide (gelatinoid silica, >99·99%). The oxygen content of the nitride powders was taken into account in computing the various compositions. These compositions were mixed in agate mortar under absolute alcohol for 2 h, dried and then isostatically pressed (400 MPa). Some compositions were prepared from synthesized compounds, such as $CaO.Al_2O_3.2SiO_2$, $2CaO.Al_2O_3.SiO_2$, $CaO.Al_2O_3$ or $CaO.6Al_2O_3$ etc., in order to check the results obtained from the starting powders mentioned above. Each composition was fired or hot-pressed at two different temperatures and then annealed by subsequent heat treatment at 1300°C for 20 h.

All as-fired and annealed specimens were analyzed by X-ray diffraction.

3 RESULTS AND DISCUSSION

Twenty nine compositions were studied with different conditions of heat treatment. Their weight losses and crystalline phases present were determined and some of these are given in Table 1. Equilibrium was assumed to have been attained when the number and type of phases did not change with different heat treatments or from different starting materials. The experimental results obtained indicate that in the specimens containing large amounts of silicon nitride, some of the α-Si_3N_4 phase could not be totally transformed to β'-Si_3N_4 even at 1700°C. Otherwise, equilibrium was readily attained in most of the compositions at 1550°C within one hour of firing time. Some compositions bloated at temperatures around 1550°C and could reach equilibrium only at temperatures below 1550°C. Because of the weight losses observed, the phase assemblages as determined by X-ray analyses were taken as an indication of the final specimens' compositions and were used for the determination of phase relationships.

The quasi-quaternary system Si, Al, Ca/N, O has three independent composition variables. Therefore, the subsolidus phase relations in the system can be represented in a triangular prism (Fig. 1), in which a four-phased field can be represented as a tetrahedron. The compatibility relationships found in this system are listed in Table 2. Graphic representation of these tetrahedra are given in Figs 2–9.

A new quinary phase (designated as S-phase) and a complete series of solid solutions between the new phase and $CaO.2Al_2O_3$ were found. The X-ray diffraction patterns of them are given in Table 3 and compared with the pattern of $CaO.2Al_2O_3$. Because of the X-ray pattern similarity and the formation of a continuous solid solution with $CaO.2Al_2O_3$, S-phase was considered to be a substituted $CaO.2Al_2O_3$ with Si–N replacing Al–O pairs. Therefore several compositions around the composition of $CaO.Al_2O_3.Si_2N_2O$ have been examined. The results are shown in Table 4. It can be seen that single phase material can be obtained up to the composition $CaO.1{\cdot}33Al_2O_3.0{\cdot}67Si_2N_2O$ (No. 4). All melted or partly melted compositions including No. 4 consisted of glass, α-Si_3N_4 and polytypoid phases such as 12H and 15R. After devitrification, all compositions, even No. 4, crystallized out as S-phase plus gehlenite. This strange behaviour of No. 4 which is shown to be a pure S-phase after being directly fired to 1400°C, may be caused by the fact that the liquid phase once formed cannot be completely devitrified. So it seems that solid state reaction is necessary to get single-phase S-phase. Compositions 1, 4 and 5 are located on the line between $CaO:2Si_2N_2O$ and $CaO:2Al_2O_3$. From X-ray analyses, it is obvious that the limit of solubility is about $CaO.1{\cdot}33Al_2O_3.0{\cdot}67Si_2N_2O$.

$CaO.6Al_2O_3$ was very difficult to form in this

Table 1. Experimental data used to establish phase relationships

No.	Composition (eq. %)					Temp. (°C)	Time (h)	W.L. (%)	Phase present	Note
	Si	Al	Ca	O	N					
1	67·26	30·13	2·60	54·47	45·53	1 550	1	3·2	X1s, Bs, αm, AlOw	
						1 300	20	*	X1s, Bs, Ams, αm, AlOw	
						HP1 500	1	/	X1m, Bm, αw, AlOm	
						1 300	20		X1m, Bm, αw, Aw	
2	54·29	42·59	3·12	59·64	40·36	1 550	1	3·6	AlOs, B30w, Bw, αw	
						1 300	20		AlOs, Am, Bmw, B30w, αw, X1vvw	
						1 700	1	17·5	B50vs, AlOmw, X1w	
						1 300	20		B50vs, Am, X1w, AlOvw	
3	83·68	12·55	3·77	30·96	69·04	1 550	1	2·5	Bs, αms, AlOmw	
						1 300	20		Bvs, αs, Am	A[b]
						1 700	1	1·7	Bvs, AlOm	
						1 300	20		Bvs, Aw, AlOvw	A[b]
4	79·43	9·41	11·16	81·19	18·81	1 550	1	12·3	SNOm, Bvw	
						1 300	20		SNOm, Bvvw	
						1 700	1	18·7	SNOm, Bvw, αvw	
						1 300	20		SNOm, Bvw, αvw	
5	61·64	20·20	18·16	81·15	18·85	1 550	1	11·6	Bvw, αvvw	
						1 300	20		Gvs, As, SNOmw, Bvw, αvw, Cvw	
						1 700	1	/	Bvvw	
						1 300	20		Gs, SNOm, Amw, Cvvw	
6	73·81	10·71	15·48	56·25	43·75	1 550	1	11·4	Bmw, αvw	
						1 300	20		Gs, Bmw, αvw	
						1 450	1	10·1	Bm, αm, AlOvvw	
						1 300	20		Gs, Bm, αmw, AlOvvw	
7	69·64	20·09	10·27	56·25	43·75	1 550	1	27·7	Bw, αw	
						1 300	20		Ams, Gm, Bm, αw, Cvw, AlOvvw	
						1 450	1	7·5	Bm, αm, AlOvvw	
						1 300	20		Am, Gm, Bmw, αmw, AlOvvw, Cvvw	
8	36·79	60·09	3·12	79·64	20·36	1 550	1	2·2	AlOvs, Bw, αw, B30vw	
						1 300	20		AlOs, Am, X1w, Bw, αw, B30vw	
						1 700	1	/	AlOs, B60m	
						1 300	20		AlOs, B60mw, Amw, X1vvw	
11	62·15	27·58	10·27	55·00	45·00	1 550	1	/	Bm, αm, B30w, AlOvw	
						1 300	20		Gs, As, Sms, Bms, αm, AlOmw, B30vvw, Cvvw	
						1 500	1	5·3	Bm, αm, AlOvw	
						1 300	20		Gms, Sms, Am, Bm, αm, AlOvw, Cvvw	
12	67·20	24·24	8·56	46·67	53·33	1 550	1	6·4	B30m, Bm, αm, A10vw	
						1 300	20		Ams, Sm, Gm, Bm, αm, B30mw, AlOw	
						1 450	1	6·3	Bm, B30mw, αmw, AlOmw	
						1 300	20		Am, Bmw, Smw, Gw, αw, AlOvw	
13	50·13	37·60	12·26	62·40	37·60	1 550	1	4·2	Sw, Bw, αvvw, AlOvvw	
						1 300	20		Ss, Gm, Aw, Bw, AlOvw	
						HP1 450	0·5	/	Sw, Bw, αw, AlOvw	
						1 300	20		Ss, Gms, Amw, Bmw, αvw, AlOvvw	

(*continued*)

Table 1—*contd.*

No.	Composition (eq. %)					Temp. (°C)	Time (h)	W.L. (%)	Phase present	Note
	Si	Al	Ca	O	N					
14	32·24	53·31	14·44	90·60	9·40	1 550	1	7·3	AlOm	
						1 300	20		Gs, AlOm, Am, Sw, Cvvw	
						1 550	1	6	AlOs	
						1 300	20		GS, A10ms, Am, Sm, Cvvw	A[b], C6A[b]
15	42·99	42·99	14·03	89·25	10·75	1 550	1	9·1	AlOvvw	
						1 300	20		As, Ss, Gm, AlOvw, Cvvw	
						1 450	1	10·1	AlOs	
						1 300	20		Ams, Gm, Sw, AlOw, Cvvw	
16	34·05	54·66	11·29	94·63	5·73	1 550	1	8·4	AlOs	
						1 300	20		AlOms, Am, Gm, Svw, Cvvw	
						1 500	1	8·4	AlOvs, Avw	
						1 300	20		AlOms, Gm, Am, Sw, Cvw	
18	36·96	52·97	10·07	92·54	7·46	1 550	1	5·9	AlOs	
						1 300	20		AlOms, Ams, Gw, Sw, Cvw, Bvvw	
						1 700	1	11	AlOw	
						1 300	20		AlOm, Am, Gw, Sw, Cvvw, Bvvw	
19	25·07	61·78	13·15	81·20	18·80	1 550	1	4·4	AlOm, Sw	
						1 300	20		Gms, AlOm, S'mw, Avw	
						HP1 450	0·5	/	S's, AlOw, Gvw	
						1 300	20		S's, AlOw, Gvw	C2A[b]
20	39·64	40·35	20·19	81·17	18·83	1 550	1	5·8	None	
						1 300	20		Gs, Sm, Aw, AlOvw	
						1 450	1	11·1	Gs	
						1 300	20		Gs, Smw, Aw, AlOvw	
29	74·21	19·67	6·10	25·35	74·65	1 550	1	5·1	B40s, Bw, αvw, AlOvw	
						1 300	20		B40vs, Bw, Sw, Aw, αvvw	
						1 700	1	5·8	B30vs, Bvw, αvvw, AlOvvw	
						1 300	20		B30vs, Sw, Aw, Bvw	

[a] Annealed at 1 300°C; all samples had a weight loss of <1%.
[b] Using pre-synthesized compounds to make the composition.
α, α-Si_3N_4; B, β-Si_3N_4; B30, β′-sialon (Z = 2·18); B40, β′-sialon (Z = 2·82); B60, β′-sialon (Z = 4·0); CA, $CaO.Al_2O_3$; C2A, $CaO.2Al_2O_3$; C6A: $CaO.6Al_2O_3$; AlO, Al_2O_3; SNO, Si_2N_2O; X1, X_1- phase; S, S-phase ($CaO.1{\cdot}33Al_2O_3.0{\cdot}67Si_2N_2O$); S′, Solid solution between S and $CaO.2Al_2O_3$; C, α-cristobalite (SiO_2); A, anorthite ($CaO.Al_2O_3.2SiO_2$); G, gehlenite ($2CaO.Al_2O_3.SiO_2$).

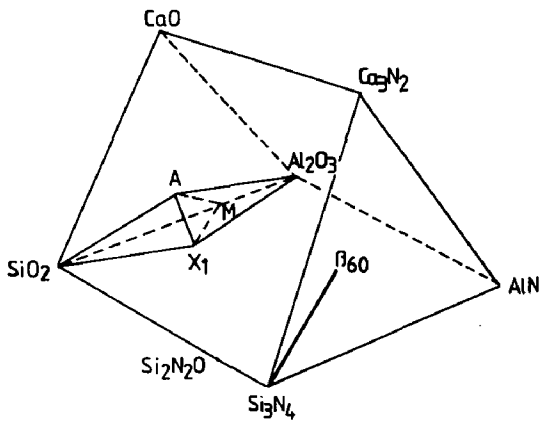

Fig. 2. Compatibility tetrahedra SiO_2–anorthite–X_1–mullite and anorthite–X_1–mullite–Al_2O_3.

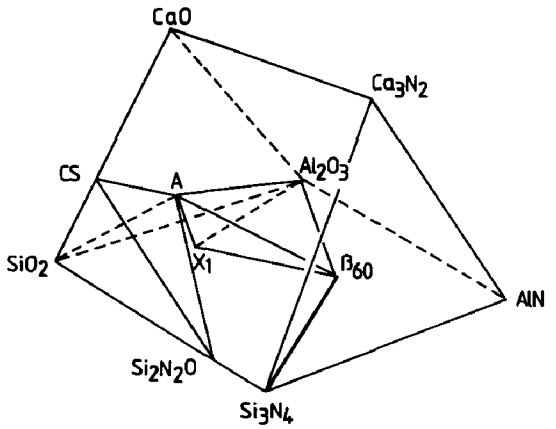

Fig. 3. Compatibility tetrahedra SiO_2–$CaSiO_3$–anorthite–Si_2N_2O and anorthite–X_1–β_{60}–Al_2O_3.

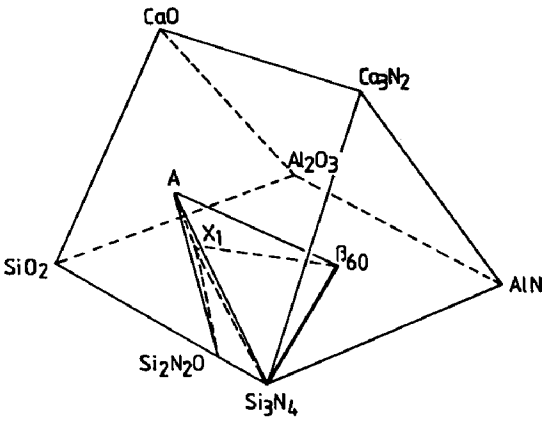

Fig. 4. Compatibility tetrahedra Si_2N_2O–anorthite–X_1–Si_3N_4 and Si_3N_4–X_1–anorthite–β_{60}.

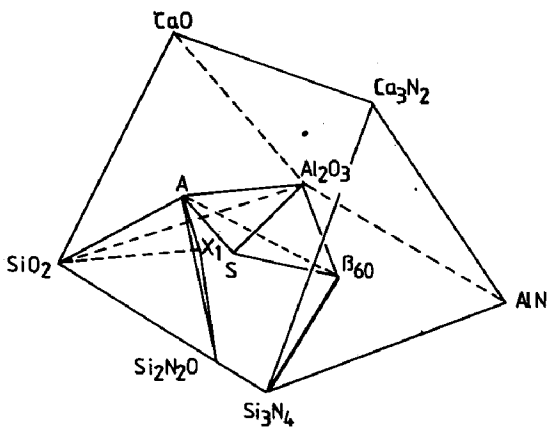

Fig. 5. Compatibility tetrahedra Si_2N_2O–SiO_2–X_1–anorthite and S–anorthite–Al_2O_3–β_{60}.

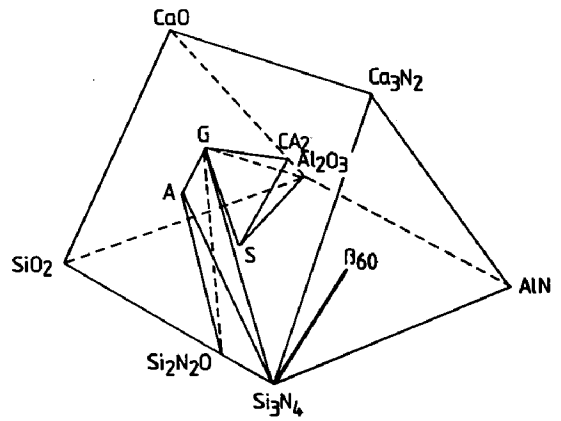

Fig. 6. Compatibility tetrahedra, Si_2N_2O–anorthite–gehlenite–Si_3N_4 and S–gehlenite–$CaO.2Al_2O_3$–Al_2O_3.

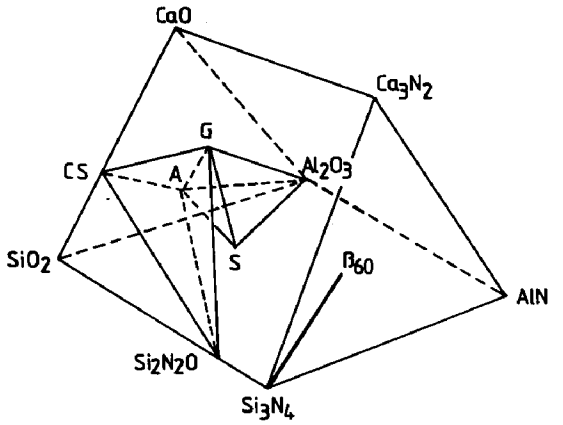

Fig. 7. Compatibility tetrahedra Si_2N_2O–$CaSiO_3$–anorthite–gehlenite and S–anorthite–gehlenite–Al_2O_3.

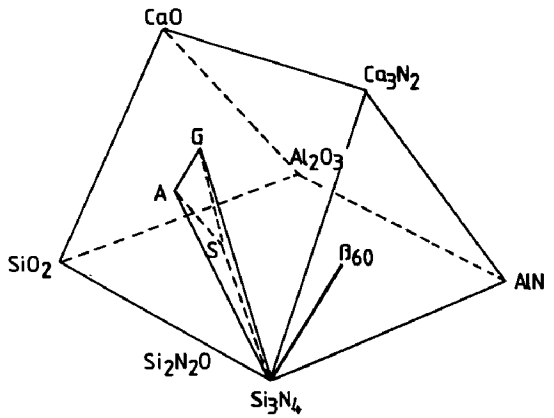

Fig. 8. Compatibility tetrahedron Si_3N_4–S–anorthite–gehlenite.

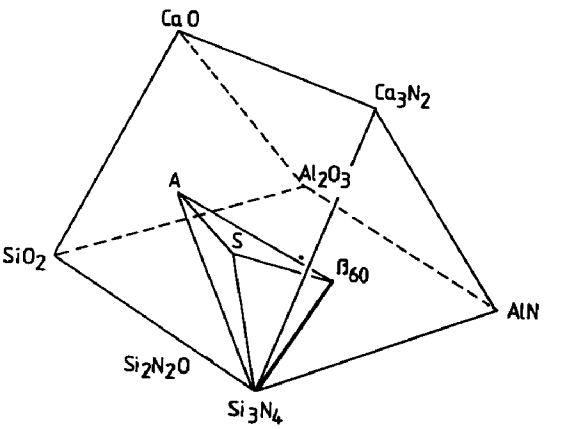

Fig. 9. Compatibility tetrahedron Si_3N_4–β_{60}–S–anorthite.

Table 2. Quaternary compatibility relationships in the system Si, Al, Ca/N, O

X_1-SiO_2–anorthite–mullite	(Fig. 2)
X_1-anorthite–mullite–Al_2O_3	(Fig. 2)
X_1-anorthite–Al_2O_3–β_{60}	(Fig. 3)
X_1-anorthite–β_{60}–Si_3N_4	(Fig. 4)
X_1-anorthite–Si_3N_4–Si_2N_2O	(Fig. 4)
X_1-anorthite–Si_2N_2O–SiO_2	(Fig. 5)
Anorthite–Si_2N_2O–SiO_2–$CaSiO_3$	(Fig. 3)
Anorthite–Si_2N_2O–$CaSiO_3$–gehlenite	(Fig. 7)
Anorthite–Si_2N_2O–gehlenite–Si_3N_4	(Fig. 6)
S-anorthite–Al_2O_3–β_{60}	(Fig. 5)
S-Al_2O_3–CaO . $2Al_2O_3$–gehlenite	(Fig. 6)
S-Al_2O_3–gehlenite–anorthite	(Fig. 7)
S-gehlenite–anorthite–Si_3N_4	(Fig. 8)
S-anorthite–Si_3N_4–β_{60}	(Fig. 9)

system even using synthesized CaO . $6Al_2O_3$ (including a small amount of Al_2O_3) as a starting material to form the compositions. The composition regions where CaO . $6Al_2O_3$ should appear always showed Al_2O_3 and/or CaO . $2Al_2O_3$ instead. CaO . $6Al_2O_3$ is an incongruent melting compound[4] and was reported as unstable in some early work.[5] Because of its absence in the system Si, Al, Ca/N, O as studied, CaO . $6Al_2O_3$ was not taken into account in establishing the compatibility phase relationships.

The compositions located in the region bounded by Si_3N_4, S-phase, $2CaO.Al_2O_3.SiO_2$, CaO . Al_2O_3, Al_2O_3 and β_{60}, where AlN or AlN polytypes appeared, were not used to establish compatibility tetrahedra, because they are beyond the region studied in this paper.

In some nitrogen-rich compositions with some proper contents of Al and Ca (compositions 9 and 10), the appearance of α'-sialon[6] was expected and was also not taken into the establishment of phase relationships concerned.

The existence of the tetrahedron S-phase-anorthite-Si_3N_4-β_{60} indicates that, in a Ca–sialon system, no crystalline compound is suitable to be used as a refractory second grain boundary phase to generate a promising β'-sialon ceramics, because of their relatively low melting points (1550°C for anorthite and 1450°C for S-phase).

4 CONCLUSIONS

Subsolidus phase relationships in the region bounded by Si_3N_4, SiO_2, $CaSiO_3$, $2CaO.Al_2O_3.SiO_2$, $CaO.Al_2O_3$, Al_2O_3 and β_{60} have been established. In this region, a new phase (S-phase) with composition near to $CaO.1{\cdot}33Al_2O_3.0{\cdot}67Si_2N_2O$ and a continuous solid solution of the new phase with $CaO.2Al_2O_3$ was found. The existence of the compatibility tetrahedron S-

Table 3. X-ray pattern of the unknown S-phase and its solid solution S_{ss}

S		S_{ss} (sample 23)		CaO . $2Al_2O_3$ (ASTM)	
d[a]	I/I_1[b]	d	I/I_1	d	I/I_1
6·18	vvw	6·25	vvw	6·16	6
				4·616	6
4·34	m	4·40	w	4·40	55
3·55	w	3·59	vw	3·60	20
3·47	vs	3·50	vs	3·50	100
				3·23	6
3·09	m	3·10	m	3·08	30
2·81	vw	2·79	vvw	2·882	20
2·74 }	s	2·75	s	2·753	25
2·73 }		2·725	s	2·712	25
2·61	s	2·61	s	2·599	60
2·55	s	2·58	s		
2·52	mw	2·53	w	2·534	15
				2·462	6
2·42	w	2·42	w	2·452	6
				2·436	16
2·34	w	2·33	w	2·404	6
				2·350	16
2·20	vw	2·19	vw	2·181	6
2·06	w	2·06	w	2·054	16

[a] d is the spacing in the lattice parameter.
[b] I/I_1 is the relative intensity of X-ray diffraction lines.

Table 4. Compositions and firing conditions explored for the preparation of pure S-phase

No.	Composition (at%)					Firing condition (°C–h)	Weight loss (%)	Phase present
	Ca	Al	Si	N	O			
1	1	2	2	2	5	1 320–0·5	1·8	Svs; Gs; αm
						1 380–0·5	1·8	αm; 12Hw
						1 450–1	2·0	αw; 12Hw
						d.1 200–45	—	Sm; Gm[a]
2	1	2	2	2·33·	4·5	1 550–1 + 1 650–1	3·7	αvw; Pvw.
						d.1 200–45	—	Ss; Gs; αvw; Pvw
3	1	2	2	2·66	4	1 500–1 + 1 650–1	0·9	α'w; Pvw
						d.1 200–45	—	Sm; Sm; αw; Pvw
4	1	2·66	1·34	1·34	5·66	1 400–0·5	3·3	Svs; α'tr.
						d.1 400–48	—	Svs[b]
						1 450–1	3·2	15Rw; 12Hvw; αtr.
						1 550–0·5	—	none
						d.1 200–45	—	Ss; Gs
5	1	2·4	1·6	1·6	5·4	1 300–0·5	1·9	Svs; Gs; αm
						1 380–0·5	1·7	12Hw

S, S-phase; G, gehlenite; α, α-Si_3N_4; α', α'-sialon; P, AlN-polytype.
[a] Phase assemblages were the same as devitrified at 1 100°C and 1 300°C.
[b] X-ray diffraction lines became sharper; 1 200°C and 1 300°C had no such effect.

phase–anorthrite–β-Si_3N_4–β_{60} implies that the fabrication of β'-sialon ceramics with a Ca-containing compound as a possible second crystalline grain boundary phase cannot be promising for high temperature applications.

REFERENCES

1. NAIK, I. K. & TIEN, T. Y., *J. Am. Ceram. Soc.*, **62**(11–12) (1979) 642.
2. SUN, W. Y., HUANG, Z. K. & CHENG, J. X., *Trans. Brit. Ceram. Soc.*, **82** (1983) 173.
3. SUN, W. Y., HUANG, Z. K., CAO, G. Z. & YAN, D. S., *Scientia Sinica* (Series A), **XXXI**(6) (1988) 742.
4. LEVIN, E. M., ROBBINS, C. K. & McMURDIE, H. F. (Eds), *Phase Diagram for Ceramists*, The American Ceramic Society, 1964.
5. GENTILE, A. L. & FOSTER, W. R., *J. Am. Ceram. Soc.*, **46**(2) (1963) 74.
6. HAMPSHIRE, S., PARK, H. K., THOMPSON, D. P. & JACK, K. H., *Nature*, **274**(5674) (1978) 880.